

Quantifying deficits in the 3D force capabilities of a digit caused by selective paralysis: application to the thumb with simulated low ulnar nerve palsy

Laurel Kuxhaus^a, Stephanie S Roach^a, Francisco J Valero-Cuevas^{a,b,*}

^aNeuromuscular Biomechanics Laboratory, Sibley School of Mechanical and Aerospace Engineering, Cornell University, Ithaca, NY 14853-7501, USA

^bLaboratory for Biomedical Mechanics and Materials, The Hospital for Special Surgery, New York, NY, USA

Accepted 13 May 2004

Abstract

We present the development of a vision-feedback method to characterize how selective paralysis distorts the three-dimensional (3D) volume representing digit-tip force production capability and its application to healthy individuals producing thumb-tip force with and without simulated low ulnar nerve palsy (LUNP). Subjects produced maximal static voluntary force spanning the transverse, sagittal and frontal planes of the thumb (16, 15 and 10 subjects, respectively). Subjects produced thumb-tip force tasks in guided and self-selected directions. The envelope (convex hull) of extreme forces in each plane approximated that cross-section of the 3D volume of force capability. Some subjects repeated the tasks with a temporary ulnar nerve block applied at the wrist to simulate complete acute LUNP. Three geometric properties of the force convex hull characterized each cross-section's shape: the ratios of its principal moments of inertia (RPMIs), the orientation of its principal axis (OPA), and its centroid location. Our results show that force production in the thumb's sagittal plane may be a reproducible and objective test to grade motor impairment in LUNP: paired *t*-tests of the larger RPMI in this plane best distinguished the nerve-blocked cases from the control cases in the *guided* task ($p = 0.012$), and Discriminant Analysis of the centroid location for the *self-selected* task in this plane correctly classified 94.7% of subjects into the control and ulnar nerve-blocked groups. We show that our method measures and detects changes in a digit's force production capabilities. Towards a clinical test of motor impairment in LUNP, this biomechanical study dictates which 3D thumb-tip forces to measure (those in the sagittal plane) and how to measure them (using the self-selected task).

© 2004 Elsevier Ltd. All rights reserved.

Keywords: Hand weakness; Peripheral neuropathy

1. Introduction

Our ability to produce digit-tip forces, especially of the thumb, in many three-dimensional (3D) directions is crucial to manipulate objects in daily activities. The weakening or loss of any hand muscle in neurological injury or disease can degrade manipulation ability. However, the biomechanical complexity of the digits hinders clinical care by making it difficult to quan-

tify motor deficits. Thus, quantifying the 3D digit-tip force production is critical to grading motor loss (and recovery) due to neurological diseases and their treatment.

The static force production capabilities of a digit-tip are fully quantified by its feasible force set (FFS), which is the 3D volume (vector space) representing maximal force production in all 3D directions (Valero-Cuevas et al., 1998; Valero-Cuevas, 2000; Valero-Cuevas and Hentz, 2002). Each digit's muscle can produce a force vector at the digit-tip (Valero-Cuevas et al., 1998; Pearlman, 2002; Valero-Cuevas and Hentz, 2002; Pearlman et al., in press), and the convex hull of all positive linear combinations of these vectors is the digit's FFS (Valero-Cuevas et al., 1998; Valero-Cuevas, 2000;

*Corresponding author. Neuromuscular Biomechanics Laboratory, Sibley School of Mechanical and Aerospace Engineering, Cornell University, 220 Upson Hall, Ithaca, NY 14853-7501, USA. Tel.: +1-605-255-3575; fax: +1-605-255-1222.

E-mail address: fv24@cornell.edu (F.J. Valero-Cuevas).

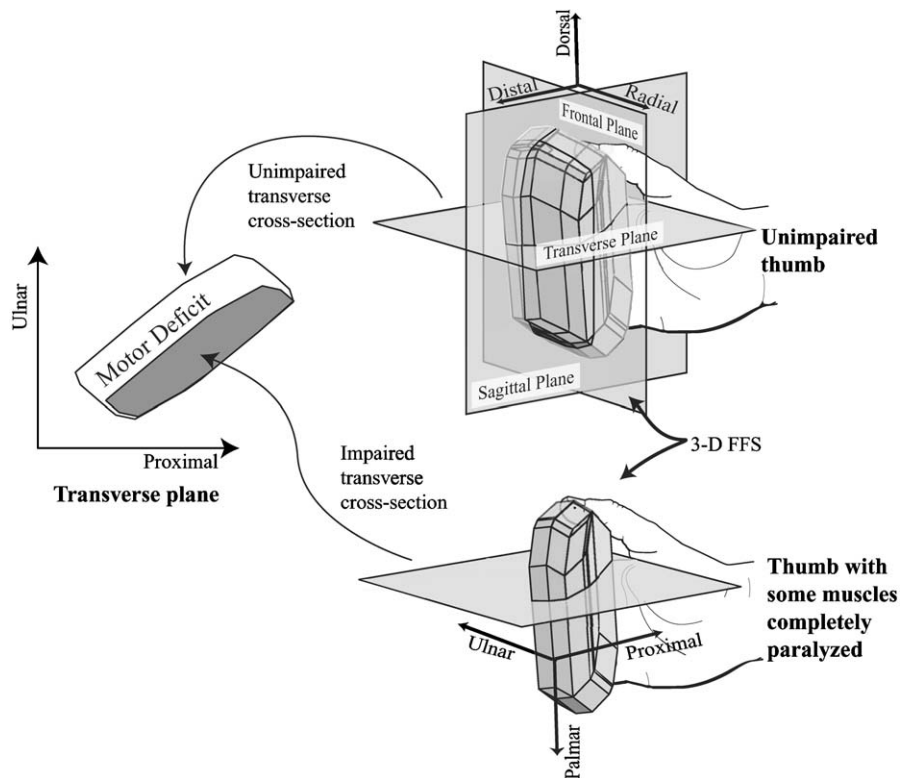


Fig. 1. Schematic of the distortion of 3D FFS with selective paralysis (based on preliminary predictions (Kuxhaus et al., 2003) from cadaver data (Pearlman et al., 2004; Pearlman, 2002) of the thenar muscles: *abductor pollicis brevis*, *opponens pollicis* and half of the *flexor pollicis brevis*. The thumbs are in Key Pinch posture. The top (unimpaired) thumb also shows the three anatomic cross-sections of the FFS, and the bottom (impaired) shows the anatomic directions. Note that from the perspective on the right, both the unimpaired and impaired FFS appear similar—much taller than they are wide. However, comparing the transverse cross-sections (on the left) reveals a motor deficit caused by the impairment.

Valero-Cuevas and Hentz, 2002; Yokogawa and Hara, 2002). The precedent logic for our hypothesis is that, because each muscle contributes uniquely to the FFS's size and shape, any muscle's impairment will distort the FFS in both size (it will shrink) and shape (it will change) (Valero-Cuevas and Hentz, 2002). We hypothesize that the shape properties of cross-sections of the FFS will change in a characteristic way that is sensitive to motor impairment in simulated low ulnar nerve palsy (LUNP), regardless of the subject's strength. In essence, we expect the relative 3D force production capabilities among muscles to be similar across subjects for a given partial paralysis because of the similarities in the direction of thumb-tip force vectors produced by each muscle (Pearlman et al., in press). Fig. 1 schematically illustrates how a cross-section of the thumb's FFS may distort with paralysis of some muscles (Kuxhaus et al., 2003).

To test this hypothesis, we developed a method to measure cross-sections of any digit's FFS and applied it to the thumb with simulated LUNP. As a first application of our method, we chose to investigate thumb-tip forces in simulated LUNP because the thumb is critical to manipulation, LUNP causes motor deficits in all digits including the thumb, the current clinical

diagnosis and evaluation of LUNP routinely include tests of thumb motor impairment, LUNP does not affect thumb sensation, and there is currently no "gold standard" to objectively and sensitively quantify thumb motor loss in LUNP (Dellon, 1989) (see Section 4). Because a minority of thumb muscles are supplied by the ulnar nerve, this study explicitly evaluates our method's ability to detect motor deficit caused by the loss of a few muscles.

2. Methods

We developed a technique to measure cross-sections of a digit's 3D FFS and applied it to the thumb. To test our hypothesis, we investigated the test-retest repeatability of measuring the transverse, sagittal and frontal cross-sections of the thumb-tip's 3D FFS (Fig. 1), and tested its sensitivity to the acute effects of severe LUNP, simulated via a temporary ulnar nerve block that impaired four of the thumb's 10 muscles (all of first dorsal interosseous, *adductor pollicis*, the deep head of *flexor pollicis brevis*, and portions of the *opponens pollicis* (Williams, 1995; Hentz and Chase, 2001)).

2.1. Experimental methods

We developed a method using vision-feedback force tasks to measure 3D thumb-tip force production capability in three planes (Kuxhaus, 2003). Subjects

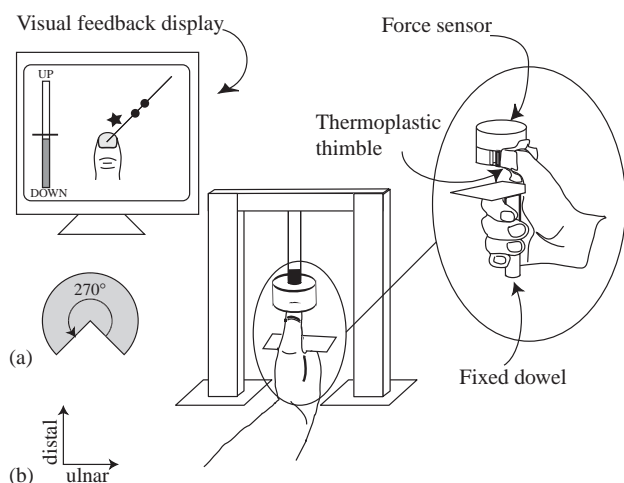


Fig. 2. Schematic of the testing apparatus and the guided task in the transverse plane. A custom thermoplastic thimble helped provide a secure and comfortable coupling to the aluminum receptacle bolted to the force sensor, which was attached to a rigid frame. Subjects were instructed to produce as much force as possible (i.e., to move the star as far as possible) in the direction of the targets (shown as circles). The targets moved radially outward along the line in response to the subject's force production (the star), and changed color and shape if the subject's force vector differed more than 10° from the targets' direction. The slider on the left indicated force production out of the plane of interest. The sketch of the thumb was included for the subject's reference, and remained stationary during the task. Inset (a) illustrates the 270° range of targets presented in this plane. Inset (b) indicates the anatomic directions associated with this plane, which were not displayed to the subject.

gripped a vertical and rigid 1.9 cm diameter dowel with the fingers (Fig. 2). To begin, we placed the thumb in Key Pinch posture (horizontal distal phalanx centered over the grasped dowel) and coupled the distal phalanx to an adjustable-height rigidly held 3D force/torque sensor (JR3 20E12A, JR3, Woodland, CA) via a custom-molded thermoplastic thimble (Spectrum, Northcoast Medical Company, Morgan Hill, CA) (Valero-Cuevas et al., 1998; Pearlman, 2002; Valero-Cuevas et al., 2003) lined with high-friction foam to prevent the thumb from slipping out of the thimble (Omnimedia Inc., New York, NY). The thimble was inserted into an aluminum receptacle bolted to the load cell and secured via cable ties which imprinted the warm thermoplastic. The thimble's fit was comfortable, yet snug enough to prevent the thumb-tip from pulling out easily. The subject's arm was loosely secured to a support mat via a Velcro™ strap. All subjects were between 20 and 50 years of age, had no history of hand or neurological dysfunction and read, understood, and signed a consent form approved by the University Committee on Human Subjects at Cornell University. Table 1 shows the subjects' descriptive statistics. We tested the dominant hand (as per the Edinburgh Handedness Inventory score, Oldfield, 1971) and both hands of one ambidextrous subject. We waited at least 24 h before re-testing subjects to mitigate the effects of low-frequency muscle fatigue (Skurvydas, 2000).

The tasks were presented to subjects as if their thumb-tip was the joystick of a simple video game in LabVIEW (National Instruments, Austin, TX) (Fig. 2). Subjects performed the tasks with visual feedback to increase the likelihood that we captured maximal voluntary force production (Graves and James, 1990). While we displayed the subject's force vector with respect to the

Table 1
Descriptive statistics for subjects: total number, sex distribution and mean age in years (standard deviation)

| Descriptive statistics | | First visit | Repeat visit | Nerve block |
|------------------------|--------------------|-------------------|-------------------|------------------|
| Transverse plane | Guided task | 17 (18 hands) | 15 (16 hands) | 5 |
| | | 10 female, 7 male | 10 female, 5 male | 3 female, 2 male |
| | | 23.0 (2.35) | 22.7 (1.91) | 22.0 (1.87) |
| | Self-selected task | 14 | 6 | 5 |
| | 9 female, 6 male | 2 female, 4 male | 3 female, 2 male | |
| | 22.7 (1.90) | 22.2 (2.23) | 22.0 (1.87) | |
| Sagittal plane | Guided task | 19 | 15 | 8 |
| | | 13 female, 6 male | 11 female, 4 male | 6 female, 2 male |
| | | 22.9 (2.73) | 22.3 (2.23) | 22.9 (2.30) |
| | Self-selected task | 14 | 6 | 5 |
| | 9 female, 5 male | 2 female, 4 male | 3 female, 2 male | |
| | 22.7 (1.90) | 22.2 (2.23) | 22.0 (2.30) | |
| Frontal plane | Guided task | 13 | 10 | 4 |
| | | 4 female, 9 male | 4 female, 6 male | 1 female, 3 male |
| | | 25.4 (7.32) | 26.7 (8.11) | 29.8 (12.7) |
| | Self-selected task | 13 | 10 | 4 |
| | 4 female, 9 male | 4 female, 6 male | 1 female, 3 male | |
| | 25.4 (7.32) | 26.7 (8.11) | 29.8 (12.7) | |

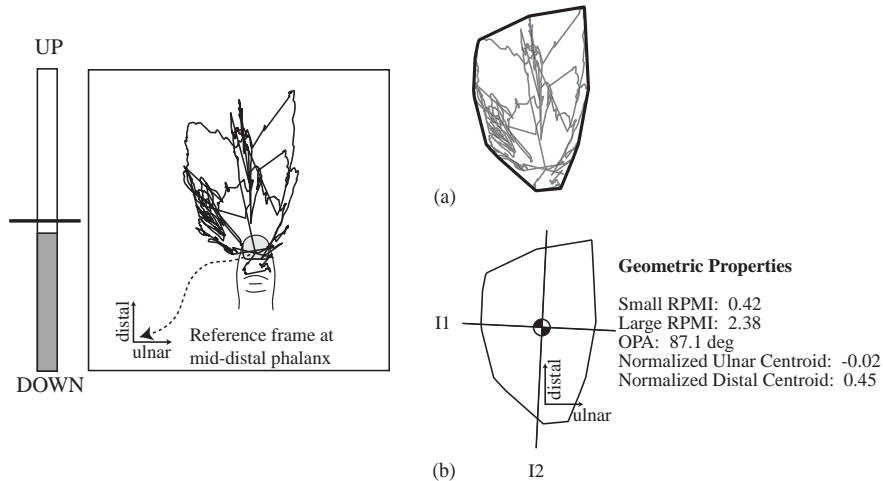


Fig. 3. Schematic of the self-selected task in the transverse plane, with one subject's complete performance and results shown. The goal of this task was for the subject to "paint" the largest planar region possible using isometric thumb-tip force. Recall that the trace of the subject's force production shows only those points which are within the 10° tolerance of the plane of interest. Note that the subject tried many times to produce force in some directions (indicated by many lines passing over the same regions of the plot). The sketch of the thumb was included for the subject's reference, and remained stationary during the task. The anatomic directions indicated are for reference and were not displayed to the subject. Inset (a) shows the convex hull (convex polygonal cross-section of the FFS) that encloses all data. Inset (b) shows the reference frame (the dashed lines), the convex hull (solid line), its centroid and principal axes (labeled I1 and I2), along with the geometric properties of the shape (OPA = orientation of the principal axis; RPMI = ratio of the principal moments of inertia). The reference distal–ulnar frame is centered in the mid-distal phalanx.

plane of interest (Fig. 2), the direction in which thumb-tip force vectors were produced was either *guided* or *self-selected*. A brief warm-up activity acquainted the subject with the tasks and their feedback. During the *guided task* we instructed subjects to maximize force magnitude in the direction of two collinear targets, which moved radially outward in the plane in response to the subject's force magnitude (Fig. 2). The targets changed shape and color if the subject's force vector (the endpoint shown as a star, Fig. 2) deviated more than 10° from the targets' 3D direction. In the frontal plane, we presented 20 equally spaced targets spanning 360° . In the sagittal and transverse planes, we presented 15 equally spaced targets spanning 270° , avoiding the mostly proximal directions that would have caused the thumb to slip out of the thimble (Fig. 2). We provided the subjects as much time as desired to complete each direction. We attenuated the effects of fatigue and learning by presenting the targets in a block-randomized order: each block consisted of a set of mutually perpendicular targets (four for the frontal plane, and three for the other two planes) in random order. We required at least 10 s rest between targets. During the *self-selected task*, we instructed subjects to "paint" the largest region possible in the desired plane until "satisfied with their performance" (Fig. 3). As feedback, the force path traced by the subject was plotted only for those points within 10° of the plane of interest. Subjects performed either all guided or all self-selected tasks first, in random order. During all tasks, we collected force data continuously at 200 samples per second and updated visual feedback

every 50 ms. Subjects were permitted extended rest periods, including withdrawal from the thimble, at any time.

To investigate the sensitivity of our test to the motor loss in LUNP, we simulated the sensorimotor loss associated with acute LUNP by injecting a temporary local anesthetic (Lidocaine, 2%) near the ulnar nerve at the wrist, proximal to Guyon's canal. This clinically standard "nerve block" administered by S.S. Roach (a hand surgeon) simulated the effects of complete acute LUNP without the physical, physiological and psychological effects associated with LUNP. To ensure the procedure's safety, subjects answered a short questionnaire about their allergy, health and medical history prior to participation. Subjects performed the tasks only after they exhibited all of the following signs of severe LUNP: clear reduction in pinch strength (mean \pm SD: $60\% \pm 17\%$), loss of little finger abduction, the inability to cross the index and middle fingers, and a positive Froment's sign. Our preparation had the advantage of preserving thumb sensation via the median nerve. Subjects were instructed not to drive or participate in activities that may put them or their hands at risk until completely recovered from the nerve block. All subjects reported (via e-mail or personal communication) complete recovery within the day, most within 2–3 h of the injection. No adverse events occurred during this study.

Each FFS cross-section was estimated by calculating the convex hull of the force data in the plane of interest. The 2D convex hull algorithm found the smallest convex polygon enclosing all the points in a planar data set

(Chvátal, 1983). For all trials, the planar data set was obtained by collapsing all force vectors within 10° of the target plane onto the target plane. Custom MATLAB routines (The MathWorks, Natick, MA) selected the data sets, calculated their convex hull and quantified the shape of the cross-sections by the following geometric measures of shape: the ratios of the principal moments of inertia (RPMIs), the orientation of the principal axis (OPA), and the normalized centroid locations of the FFS cross-sections in each of the anatomic reference planes (Fig. 3).

2.2. Statistical Analysis

For all tasks in all planes, the *agreement* between the task modalities (how similar the two cross-sections from the same subject on the same day are), *test-retest repeatability* (how similar the cross-sections for the same subject and the same task are from day to day), and *sensitivity* (the ability to distinguish control from the nerve-blocked trials) were investigated. Because we seek to develop a clinically useful test (the most informative

plane, task style and geometric property), we grouped the data by plane/task combinations for all analyses. We performed all statistical analyses in SPSS (SPSS Inc., Chicago, IL). Following Bland and Altman (1986), we investigated task agreement and repeatability. Paired *t*-tests assessed each geometric property's sensitivity to LUNP. Statistical significance was set at the $\alpha = 0.05$ level. We used Discriminant Analysis to test our measures' ability to classify individuals into control and nerve-blocked groups. This parametric analysis classified each subject into the control (unimpaired) and nerve-block groups, based on the linear combination of factors that best divided the subjects into the known groups (Sokal and Rohlf, 1995). To allow for comparisons among subjects, we normalized centroid locations of the FFS cross-sections in each plane by the largest force magnitude in that plane. This analysis found the "dividing line" that best separated subjects into the control or nerve-blocked groups, in essence separating the groups independently of the coordinate system in which they are described (Sokal and Rohlf, 1995).

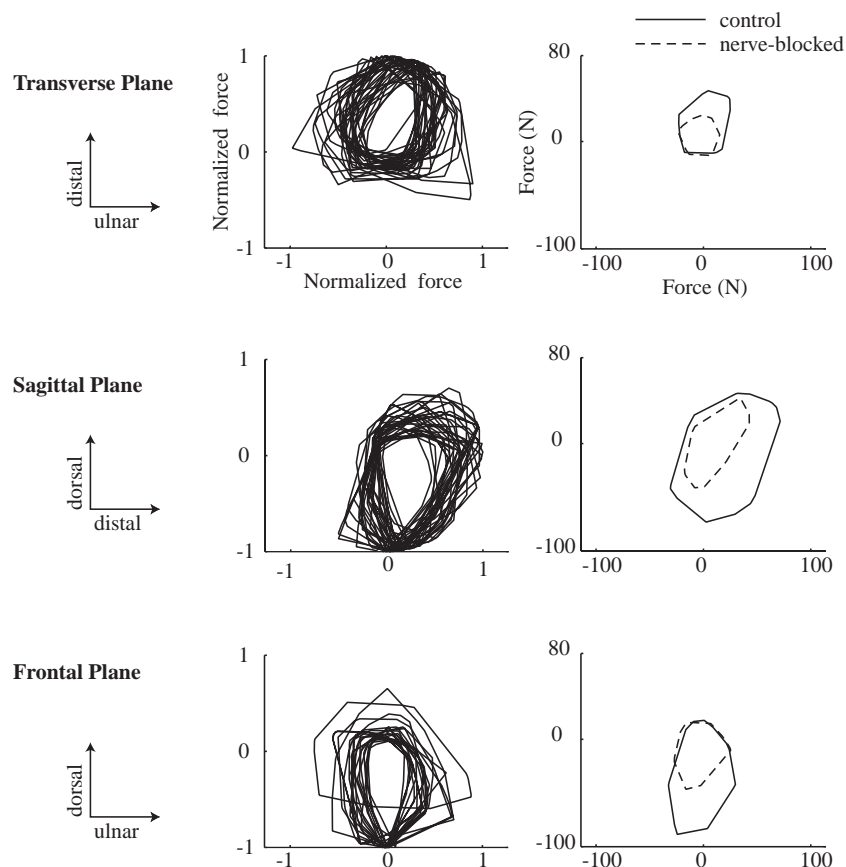


Fig. 4. Force production in each plane for the *guided task*. The left column of figures shows all of the normalized FFS cross-sections for all subjects. Note the general trends in shape apparent in each group. The right column of figures shows an example of changes caused by the nerve block for each task in each plane. Each of these shows one representative subject's unimpaired and nerve-blocked performances. Note that in the transverse plane, the nerve block produces a more circular cross-section; in the sagittal plane, a more oblong cross-section, and in the frontal plane, the nerve-blocked cross-sections are smaller in the palmar direction.

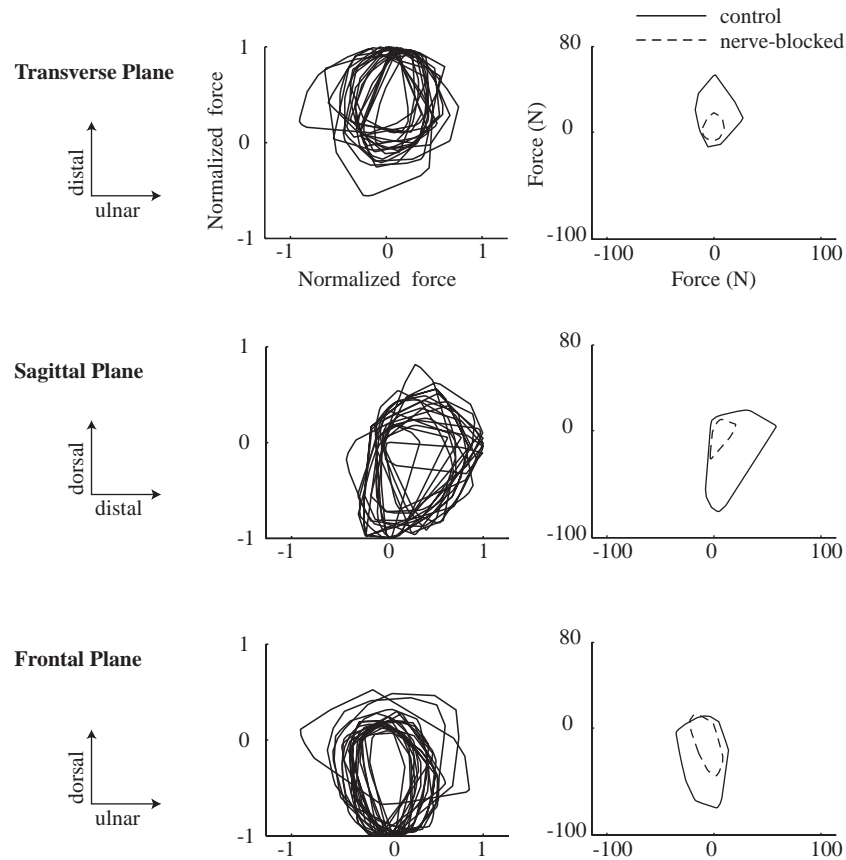


Fig. 5. Force production from each plane and for the *self-selected* task. The left column of figures shows all of the normalized FFS cross-sections for all subjects. Note the general trends apparent in each group. The right column of figures shows an example of changes produced by the nerve block for each task in each plane. Each of these shows one subject's unimpaired and nerve-blocked performances. Note that in the transverse plane, the nerve block produces a more circular cross-section; in the sagittal plane, the changes produce more oblong cross-sections, and in the frontal plane, the nerve-blocked cross-sections are smaller in the palmar direction. The few cases in which the force production boundary for the nerve-blocked case appears to exceed that of the control case are likely explained by slight day-to-day misalignment of the thumb relative to the sensor, or a possible learning effect. We do not expect that the nerve block would have increased a subject's force production capabilities in any directions.

3. Results

Our results for all planes and task combinations are displayed as follows: Figs. 4 and 5 show the normalized convex hulls from all control trials, and representative examples of the distortions produced by the nerve block; Table 2 contains the means and standard deviations for each geometric outcome; Table 3 summarizes their agreement, repeatability and sensitivity; and Table 4 shows the Discriminant Analysis results.

3.1. Transverse plane

The geometric outcomes are in good agreement for the guided and self-selected tasks (Table 3). The guided task in the transverse plane is repeatable for the RPMIs, the OPA and the ulnar centroid component. Regarding sensitivity, the distal and ulnar centroid components distinguish between the control and nerve-blocked cases. The *self-selected* task in this plane is

repeatable for the large and small RPMIs, the OPA the distal component of the centroid and the ulnar component of the centroid. The ulnar centroid component distinguishes between the control and nerve-blocked cases.

3.2. Sagittal plane

The two tasks (guided and self-selected) are in good agreement in the sagittal plane (Table 3). The *guided* task in this plane is repeatable for the large and small RPMIs, the OPA, and the distal and dorsal centroid components. The large and small RPMIs and the distal and dorsal centroid components distinguish between the control and nerve-blocked cases. The *self-selected* task in the sagittal plane is repeatable in large and small RPMI, OPA, and the distal and dorsal centroid components. The distal and dorsal centroid components distinguish between the control and nerve-blocked cases.

Table 2

Mean (standard deviation) for the geometric properties of the FFS cross-sections for all planes, both tasks

| Plane and condition | Task | Large RPMI (N^4) | Small RPMI (N^4) | OPA (degrees) | Normalized ulnar centroid component | Normalized distal centroid component | Normalized dorsal centroid component |
|---------------------------|---------------|----------------------|----------------------|----------------|-------------------------------------|--------------------------------------|--------------------------------------|
| Transverse, control | Guided | 0.51 (0.17) | 2.24 (0.86) | 69.71 (34.24) | 0.071 (0.11) | 0.34 (0.069) | n/a |
| | Self-selected | 0.59 (0.24) | 2.13 (1.23) | 94.57 (53.24) | 0.035 (0.11) | 0.41 (0.069) | n/a |
| Transverse, nerve-blocked | Guided | 0.67 (0.20) | 1.60 (0.48) | 81.17 (67.80) | -0.067 (0.045) | 0.26 (0.038) | n/a |
| | Self-selected | 0.66 (0.17) | 1.61 (0.43) | 66.36 (34.32) | -0.082 (0.13) | 0.29 (0.13) | n/a |
| Sagittal, control | Guided | 0.40 (0.13) | 2.75 (0.83) | 89.76 (61.56) | n/a | 0.25 (0.064) | -0.23 (0.066) |
| | Self-selected | 0.34 (0.18) | 4.40 (3.66) | 83.76 (33.51) | n/a | 0.30 (0.10) | -0.20 (0.10) |
| Sagittal, nerve-blocked | Guided | 0.26 (0.08) | 4.34 (1.78) | 50.72 (20.81) | n/a | 0.22 (0.10) | -0.076 (0.12) |
| | Self-selected | 0.29 (0.14) | 4.90 (3.92) | 56.77 (5.94) | n/a | 0.21 (0.11) | -0.034 (0.12) |
| Frontal, control | Guided | 0.39 (0.17) | 3.34 (2.13) | 151.90 (66.43) | 0.023 (0.040) | n/a | -0.33 (0.078) |
| | Self-selected | 0.41 (0.16) | 2.87 (1.47) | 166.09 (49.11) | 0.023 (0.062) | n/a | -0.32 (0.090) |
| Frontal, nerve-blocked | Guided | 0.41 (0.27) | 3.74 (2.86) | 3.74 (2.86) | -0.092 (0.069) | n/a | -0.21 (0.084) |
| | Self-selected | 0.42 (0.26) | 3.49 (2.54) | 1.95 (0.78) | -0.055 (0.075) | n/a | -0.27 (0.11) |

“n/a” indicates “not applicable” in the sense that centroid component does not exist for the specified plane

3.3. Frontal plane

The two tasks (guided and self-selected) are in good agreement in the frontal plane (Table 3). The *guided* task in this plane is repeatable in the large and small RPMIs, OPA, and the dorsal and ulnar centroid components. The *self-selected* task in this plane is repeatable for large and small RPMI, OPA, and both the dorsal and ulnar centroid components. The dorsal centroid component distinguishes between the control and nerve-blocked cases.

The Discriminant Analysis shows that centroid location in the plane is the outcome measure that best distinguishes between control and nerve block groups (underlined entries in rightmost column, Table 4). Fig. 6 shows the centroid locations in each plane and the line which best divides the data in two groups. Table 4 shows the correct and incorrect classifications. Centroid components for the self-selected task in the sagittal plane are the most successful (94.7% correct classifications). Most incorrect classifications are false positives.

4. Discussion

Our goal was to create a method that can be developed in to a clinically useful objective test of digit motor impairment caused by peripheral neuropathies affecting a subset of muscles. To test our hypothesis, we elected to measure thumb-tip force production in the transverse, sagittal and frontal cross-sections of the FFS because these planes are easily described to and discussed with patients and clinicians. We evaluated

the sensitivity of our technique to simulated worst-case LUNP. In essence, our tests extend the principles of pinch meters and Froment’s sign (which indicate weakening of thumb-tip force production in one direction due to selective paralysis) by evaluating thumb-tip force production in multiple directions in 3D. Because each muscle uniquely contributes to the FFS’s size and shape, our approach provides a mechanically rigorous characterization of the selective weakening of some muscles that is simple to perform, repeatable (giving the same result for the same person regardless of time), sensitive (able to detect impairment), and more informative of motor impairment than current clinical tests thumb function. The good ($\alpha = 0.05$) agreement between the guided and self-selected tasks is clinically noteworthy—as the self-selected task is shorter and less fatiguing, we believe it has the greatest potential to become a practical and useful clinical test to quantify thumb motor loss in LUNP.

Our study is limited in that our subjects are likely younger than the clinical LUNP population, and adults weaken with age (Mathiowetz et al., 1985); our temporary ulnar nerve block, conducted per current clinical standards, acutely simulates sensorimotor loss in severe LUNP; and we cannot say whether the motor deficit variability is due to our nerve block technique, innervation variability, neurological adaptation or their combination. In addition, the injection location at the wrist is near the median nerve and two subjects reported minor affected sensation in median innervated skin patches not on the thumb. To minimize our protocol’s invasiveness, we did not monitor motor loss via intramuscular electrodes in these small and sometimes

Table 3
Measures of agreement, repeatability and sensitivity (per *t*-tests) for both tasks in all three planes

| Measure | Plane | Task | Agreement | Repeatability | Sensitivity (<i>t</i> -test) |
|--------------------------------------|------------|---------------|-----------|---------------|-------------------------------|
| Small RPMI | Transverse | Guided | Yes | 0.67* | 0.66 |
| | | Self-selected | Yes | 0.16* | 0.64 |
| | Sagittal | Guided | Yes | 0.70* | 0.012* |
| | | Self-selected | Yes | 0.14* | 0.25 |
| | Frontal | Guided | Yes | 0.006 | 0.71 |
| | | Self-selected | Yes | 0.40* | 0.86 |
| Large RPMI | Transverse | Guided | Yes | 0.67* | 0.7 |
| | | Self-selected | Yes | 0.16* | 0.47 |
| | Sagittal | Guided | Yes | 0.38* | 0.0075* |
| | | Self-selected | Yes | 0.090* | 0.3 |
| | Frontal | Guided | Yes | 0.38 | 0.86 |
| | | Self-selected | Yes | 0.91* | 0.49 |
| OPA | Transverse | Guided | Yes | 0.82* | 0.49 |
| | | Self-selected | Yes | 0.25* | 0.39 |
| | Sagittal | Guided | Yes | 0.10* | 0.1 |
| | | Self-selected | Yes | 0.15* | 0.15 |
| | Frontal | Guided | Yes | 0.99* | 0.39 |
| | | Self-selected | Yes | 0.34* | 0.35 |
| Normalized ulnar centroid component | Transverse | Guided | Yes | 0.50* | 0.031* |
| | | Self-selected | Yes | 0.62* | 0.12 |
| | Sagittal | Guided | n/a | n/a | n/a |
| | | Self-selected | n/a | n/a | n/a |
| | Frontal | Guided | Yes | 0.081* | 0.094 |
| | | Self-selected | Yes | 0.34* | 0.89 |
| Normalized distal centroid component | Transverse | Guided | Yes | 0.012 | 0.011* |
| | | Self-selected | Yes | 0.27* | 0.0021* |
| | Sagittal | Guided | Yes | 0.65* | 0.0016* |
| | | Self-selected | Yes | 0.14* | 0.0052* |
| | Frontal | Guided | n/a | n/a | n/a |
| | | Self-selected | n/a | n/a | n/a |
| Normalized dorsal centroid component | Transverse | Guided | n/a | n/a | n/a |
| | | Self-selected | n/a | n/a | n/a |
| | Sagittal | Guided | Yes | 0.89* | 0.022* |
| | | Self-selected | Yes | 0.19* | 0.043* |
| | Frontal | Guided | Yes | 0.44* | 0.0034* |
| | | Self-selected | Yes | 0.39* | 0.00060* |

Note: “Agreement” is a measure of similarity between the outcomes for the two task modalities; a “yes” indicates that the outcome measures were not significantly different ($\alpha=0.05$), and suggests that both tasks equivalently measure the maximal force production capabilities of the thumb. “Repeatability” compares each subject’s test–retest performances, thus a high *p*-value (i.e., 70.05, indicated by an*) indicates NO significant difference between performances, and a “repeatable” task. “Sensitivity” compares each subject’s nerve-blocked and unimpaired performances, thus a low *p*-value (i.e., 70.05, indicated by an*) indicates the effect of the nerve block is significant. n/a indicates “not applicable” in the sense that the centroid component does not exist for the specified plane, thus its Sensitivity and repeatability cannot be assessed.

deep target muscles. Future studies could include electrophysiological tests to ensure the selectivity and homogeneity of the nerve blocks. While we imposed no external controls for shoulder and wrist posture (subjects achieve greater forces in self-selected postures, (O’Driscoll et al., 1992)), wrist radial–ulnar deviation and forearm supination were controlled as the subjects grasped the perpendicular dowel while keeping the distal phalanx of the thumb horizontal. As subjects kept this internally consistent thumb posture, we assumed that muscle fascicle length and moment arms remained

consistent across trials. Our large number of simultaneous *t*-test comparisons does not affect our conclusions about the sagittal plane given that the Discriminant Analysis independently confirms that the sagittal plane best detects impairment. Future work can test the centroids’ distribution patterns and strengthen our results. Despite the good agreement between tasks, the Discriminant Analysis percentage of correct classifications (Table 4) differs between them, perhaps due to muscle coordination variations between the two tasks (e.g., sensorimotor integration differs across feedback

Table 4
Discriminant analysis sensitivity

| Measure | Plane | Task | Percent correct | Known group | Predicted group | |
|---------------------|------------|---------------|-----------------|---------------|-----------------|---------------|
| | | | | | Control | Nerve-blocked |
| Small RPMI | Transverse | Guided | 66.7 | Control | 68.4 | 31.6 |
| | | | | Nerve-blocked | 40.0 | 60.0 |
| | | Self-Selected | 47.4 | Control | 50.0 | 50.0 |
| | | | | Nerve-blocked | 60.0 | 40.0 |
| | Sagittal | Guided | 66.7 | Control | 63.2 | 36.8 |
| | | | | Nerve-blocked | 25.0 | 75.0 |
| | | Self-selected | 52.6 | Control | 57.1 | 42.9 |
| | | | | Nerve-blocked | 60.0 | 40.0 |
| | Frontal | Guided | 41.2 | Control | 38.5 | 61.5 |
| | | | | Nerve-blocked | 50.0 | 50.0 |
| | | Self-selected | 70.6 | Control | 69.2 | 30.8 |
| | | | | Nerve-blocked | 25.0 | 75.0 |
| Large RPMI | Transverse | Guided | 54.2 | Control | 47.4 | 52.6 |
| | | | | Nerve-blocked | 20.0 | 80.0 |
| | | Self-selected | 63.2 | Control | 71.4 | 28.6 |
| | | | | Nerve-blocked | 60.0 | 40.0 |
| | Sagittal | Guided | 74.1 | Control | 84.2 | 15.8 |
| | | | | Nerve-blocked | 50.0 | 50.0 |
| | | Self-selected | 68.4 | Control | 78.6 | 21.4 |
| | | | | Nerve-blocked | 60.0 | 40.0 |
| | Frontal | Guided | 58.8 | Control | 61.5 | 38.5 |
| | | | | Nerve-blocked | 50.0 | 50.0 |
| | | Self-selected | 58.8 | Control | 53.8 | 46.2 |
| | | | | Nerve-blocked | 25.0 | 75.0 |
| OPA | Transverse | Guided | 62.5 | Control | 63.2 | 36.8 |
| | | | | Nerve-blocked | 40.0 | 60.0 |
| | | Self-selected | 57.9 | Control | 57.1 | 42.9 |
| | | | | Nerve-blocked | 40.0 | 60.0 |
| | Sagittal | Guided | 66.7 | Control | 52.6 | 47.4 |
| | | | | Nerve-blocked | 0.0 | 100.0 |
| | | Self-selected | 63.2 | Control | 50.0 | 50.0 |
| | | | | Nerve-blocked | 0.0 | 100.0 |
| | Frontal | Guided | 70.6 | Control | 84.6 | 15.4 |
| | | | | Nerve-blocked | 75.0 | 25.0 |
| | | Self-selected | 29.4 | Control | 7.7 | 92.3 |
| | | | | Nerve-blocked | 0.0 | 100.0 |
| Centroid Components | Transverse | Guided | 87.5 | Control | 84.2 | 15.8 |
| | | | | Nerve-blocked | 0.0 | 100.0 |
| | | Self-selected | 89.5 | Control | 84.2 | 15.8 |
| | | | | Nerve-blocked | 0.0 | 100.0 |
| | Sagittal | Guided | 85.2 | Control | 94.7 | 5.3 |
| | | | | Nerve-blocked | 37.5 | 62.5 |
| | | Self selected | 94.7 | Control | 100.0 | 0.0 |
| | | | | Nerve-blocked | 20.0 | 80.0 |
| | Frontal | Guided | 94.1 | Control | 100.0 | 0.0 |
| | | | | Nerve-blocked | 25.0 | 75.0 |
| | | Self-selected | 82.4 | Control | 92.3 | 7.7 |
| | | | | Nerve-blocked | 50.0 | 50.0 |

Note: Data expressed as a percentage of the total number classified. The centroid's "worst" classification rate was 82.4%, which is higher than the best success rate of any other geometric property, as indicated by the bold numbers. Note that for the centroid, many of the incorrect classifications placed a subject known to be unimpaired into the nerve block group (a false positive).

modalities and task goals, (Henningsen et al., 1997; Blakemore et al., 1998)), or due to the groups' unequal sizes. With the Discriminant Analysis, most incorrect classifications place a control subject in the nerve block

group (Table 4). These instances could be false positives or results of an imperfect normalization (e.g., a subject's maximal force used in the normalization was not their "true" physiologic maximum). In addition, the unba-

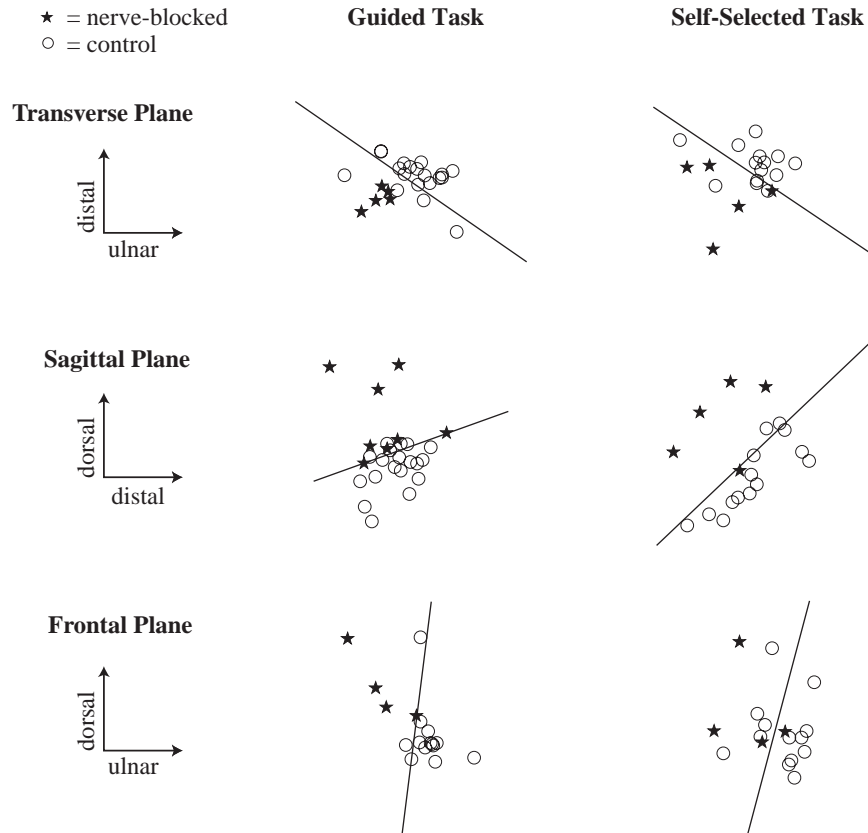


Fig. 6. Discriminant Analysis results for the normalized centroid locations for both tasks in all planes. (The centroids have been normalized by each subject's maximal force production in any planar direction.) The discriminant function lines shown divide the total population into control and nerve-blocked groups.

lanced population sizes of the nerve block and control groups may have influenced the “dividing lines”. Future work can study the effects of our analysis choice on the results.

Nevertheless, as we hypothesized, our results show that at least one cross-section (the sagittal plane) of the FFS is sensitive to motor impairment in LUNP, suggesting that force measurements in this plane may be able to quantify LUNP (Table 4) severity better than current clinical tests. The sensitivity of maximal 3D thumb-tip forces in this plane to simulated LUNP is consistent with what we know about the thumb-tip forces produced by ulnarly innervated muscles of the thumb: the *adductor pollicis*, first *dorsal interosseous*, *flexor pollicis brevis* (deep head) and *opponens pollicis* (portions of) contribute to thumb-tip force in the distal and palmar directions in the sagittal plane (Pearlman, 2002; Pearlman et al., 2004).

Discriminant Analysis of centroid locations in the sagittal plane seems the most effective and clinically promising means to classify LUNP patients. The Discriminant Analysis of all other outcome measures was $\leq 74.1\%$ successful, contrasted with a minimum of 82.4% correct classifications for the centroid locations, with the sagittal plane having the highest success rate

(94.7%) for the self-selected task. Moreover, our results are clinically encouraging because the centroid of the cross-section for the *self-selected* task (shorter and less fatiguing) distinguishes better between the control and nerve-blocked groups than the *guided* task. These results suggest our future work should focus on testing additional control subjects and patients with a shortened protocol limited to the self-selected task in sagittal plane. Clinically, these expanded baseline data may allow us to define a “transition region” where the discriminating line tends to lie, and thus categorize subsequent patients as *borderline* (i.e. in the transition region); or as clearly *unimpaired* or *impaired* (i.e., on either side of the transition region). In addition, a patient's impairment level could be graded by the distance from the transition region (i.e., how close they are to being classified as borderline).

Our work is clinically relevant to LUNP because the lack of a “gold standard” to objectively and sensitively quantify motor loss (Dellon, 1989; Tetro and Pichora, 1996) makes it difficult to select the timing and treatment choice. The typical sensorimotor deficits in LUNP degrade a person's ability to perform the activities of daily living (Osterman and Kitay, 1996; Tetro and Pichora, 1996). Left untreated, symptoms can

progress to irreversible denervation of some hand muscles, worsening the prognosis of any intervention. Thus, the application time and treatment choice is critical (Tetro and Pichora, 1996). Clinicians today need a reliable, objective, and sensitive assessment of motor impairment and recovery. Currently, to grade motor impairment for degenerative neuropathies of the hand clinicians must assemble and interpret a constellation of subjective patient questionnaires, sensory evaluations, and limited measurements of strength (Dellon, 1989).

We chose to study the thumb in simulated LUNP because, even if only four thumb muscles are supplied by the ulnar nerve, thumb pinch strength and Froment's sign are two standard motor tests used to evaluate ulnar nerve impairment (Dellon, 1989; Tetro and Pichora, 1996) (see Section 1). Pinch strength measurements are limited in that, in Key Pinch posture, a pinch meter measures thumb-tip force production only in the "palmar" direction (Fig. 1), and is insensitive to muscle impairments affecting force production in the thumb's distal-ulnar (transverse) plane (Fig. 1). Froment's sign (flexion of the distal thumb phalanx to hold a piece of paper against the hand) is a clinically accepted indicator of motor dysfunction in LUNP (Osterman and Kitay, 1996). However, Froment's sign cannot detect gradual motor loss or functional recovery because it is binary (either "positive" or "negative"), not apparent until severe motor loss has occurred, and—like pinch meters—tests force production in only one direction. We believe our approach to quantify thumb 3D force capabilities is clinically applicable and relevant to LUNP by complementing and extending current tests of thumb motor function with a sensitive (i.e., non-binary) means to quantify 3D thumb-tip force production (and deficits). Naturally, our approach is applicable to quantify motor deficits in any digit due to other neuropathies (e.g., carpal tunnel syndrome) that are beyond the scope of this first study.

We conclude that our novel test to quantify 3D digit-tip force production is objective and sensitive to the effects of LUNP on the thumb. We have not developed a ready-to-deploy clinical test as such. Rather, we have laid the engineering and scientific foundation for future studies of LUNP: we have defined what to measure (force output in the sagittal plane) and how to measure it (using the *self-selected* task). We have established a foundation upon which to refine our method and testing apparatus to produce a clinically useful tool to objectively and sensitively grade impairment and recovery in peripheral neuropathies.

Acknowledgements

The authors gratefully acknowledge Matt Maslanka, Jonathan L. Pearlman and Madhusudhan Venkadesan

for assistance in creating figures; Dr. M.G. Peterson for her assistance with the statistical analysis, and Drs. A. Ruina and T. Wright for their critical comments on earlier versions of this work. This work is supported by a Bioengineering Research Grant from the Whitaker Foundation. This material is based upon work supported under a National Science Foundation Graduate Research Fellowship (LK) and career Award Grant No. 0237258(FVC).

References

- Blakemore, S.J., Goodbody, S.J., Wolpert, D.M., 1998. Predicting the consequences of our own actions: the role of sensorimotor context estimation. *Journal of Neuroscience* 18, 7511–7518.
- Bland, J.M., Altman, D.G., 1986. Statistical methods for assessing agreement between two methods of clinical measurement. *Lancet* 1, 307–310.
- Chvátal, V., 1983. *Linear Programming*. W.H. Freeman and Company, New York.
- Dellon, A.L., 1989. Review of treatment results for ulnar nerve entrapment at the elbow. *Journal of Hand Surgery (American)* 14, 688–700.
- Graves, J.E., James, R.J., 1990. Concurrent augmented feedback and isometric force generation during familiar and unfamiliar muscle movements. *Research Quarterly for Exercise and Sport* 61, 75–79.
- Henningsen, H., Knecht, S., Ende-Henningsen, B., 1997. Influence of afferent feedback on isometric fine force resolution in humans. *Experimental Brain Research* 113, 207–213.
- Hentz, V.R., Chase, R.A., 2001. *Hand Surgery: a Clinical Atlas*. W.B. Saunders, Philadelphia, PA.
- Kuxhaus, L., 2003. *Changes in Thumb 3D Force Production with Selective Paralysis*. Cornell University, Ithaca, NY.
- Kuxhaus, L., Pearlman, J., Weisman, M., Valero-Cuevas, F.J., 2003. Predicting Thumb Force Changes with Ulnar Nerve Impairment. *American Society of Biomechanics*, Toledo, OH.
- Mathiowetz, V., Rennells, C., Donahoe, L., 1985. Effect of elbow position on grip and key pinch strength. *Journal of Hand Surgery (American)* 10, 694–697.
- O'Driscoll, S., Horii, E., Ness, R., Cahalan, T., Richards, R., An, K., 1992. The relationship between wrist position, grasp size, and grip strength. *Journal of Hand Surgery (American)* 17, 169–177.
- Oldfield, R., 1971. The assessment and analysis of handedness: the Edinburgh inventory. *Neuropsychologia* 9, 97–113.
- Osterman, A., Kitay, G., 1996. Compression neuropathies: ulnar. In: Peimer, C. (Ed.), *In Surgery of the Hand and Upper extremity*. McGraw-Hill, New York, pp. 1339.
- Pearlman, J., 2002. *The fundamental actions of the individual muscles of the thumb*. Cornell University, Ithaca, NY.
- Pearlman, J., Roach, S., Valero-Cuevas, F., 2004. The fundamental thumb-tip force vectors produced by the muscles of the thumb. *Journal of Orthopedic Research* 22, 306–312.
- Skurvydas, A., 2000. Low frequency fatigue and muscle endurance after performing intermittent eccentric exercise and continuous eccentric-concentric exercise. *Sport* 4, 46–50.
- Sokal, R., Rohlf, F., 1995. *Biometry: the Principles and Practice of Statistics in Biological Research*. Freeman, New York.
- Tetro, A.M., Pichora, D.R., 1996. Cubital tunnel syndrome and the painful upper extremity. *Hand Clinics* 12, 665–677.
- Valero-Cuevas, F.J., 2000. Predictive modulation of muscle coordination pattern magnitude scales fingertip force magnitude over the voluntary range. *Journal of Neurophysiology* 83, 1469–1479.

- Valero-Cuevas, F.J., Hentz, V.R., 2002. Releasing the A3 pulley and leaving flexor superficialis intact increases pinch force following the Zancolli lasso procedure to prevent claw deformity in the intrinsic palsied finger. *Journal of Orthopedic Research* 20, 902–909.
- Valero-Cuevas, F.J., Zajac, F.E., Burgar, C.G., 1998. Large index-fingertip forces are produced by subject-independent patterns of muscle excitation. *Journal of Biomechanics* 31, 693–703.
- Valero-Cuevas, F.J., Johanson, M.E., Towles, J.D., 2003. Towards a realistic biomechanical model of the thumb: the choice of kinematic description may be more critical than the solution method or the variability/uncertainty of musculoskeletal parameters. *Journal of Biomechanics* 36, 1019–1030.
- Williams, P.L., 1995. In: Williams, P.L. (Ed.), *Gray's Anatomy the Anatomical Basis of Medicine and Surgery*. Churchill Livingstone, New York.
- Yokogawa, R., Hara, K., 2002. Measurement of distribution of maximum index-fingertip force in all directions at fingertip in flexion/extension plane. *Journal of Biomechanical Engineering* 124, 302–307.